(19) W. J. Hehre, R. Ditchfield, L. Radom, and J. A. Pople, *J. Am. Chem. Soc.*, **92**, 4796 (1970).
(20) Strausz et al. have previously reported a similar geometry for the singlet state of formylmethylene.[11d] Their prediction of a singlet ground state for this system, and similarly for methylmethylene in the calculations[11c] of Altmann, Csizmadia, and Yates, may well be due to the use of singlet state molecular orbitals to represent T_1, thereby biasing strongly the calculations in favor of the former.
(21) (a) R. S. Hutton, M. L. Manion, H. D. Roth, and E. Wasserman, *J. Am. Chem. Soc.*, **96**, 4680 (1974). (b) At the suggestion of a referee, we have investigated the effect of including d orbitals on the oxygen atom in HCCHO. Adding $d\sigma$ and $d\pi$ orbitals to the minimal s,p basis set raises the T_1–S_0 gap by 0.5 and 0.0 kcal mol^{-1}, respectively; thus polarization functions on the oxygen are *not* important in determining the energy gap.
(22) The C–H distances in the S_0 and T_1 states were held constant at 1.13 and 1.09 Å, respectively, in these calculations.

Electronic States of the NiO Molecule[1,2]

Stephen P. Walch and W. A. Goddard III*

Contribution No. 5521 from the Arthur Amos Noyes Laboratory of Chemical Physics, California Institute of Technology, Pasadena, California 91125.
Received February 28, 1977

Abstract: Generalized valence bond and configuration interaction wave functions have been obtained as a function of R for numerous electronic states of NiO. All the lower states are found to involve the $(4s)^1(3d)^9$ Ni atom configuration and O in the $(2s)^2(2p)^4$ configuration. There are two groups of states. The lower group of states involves pairing singly occupied Ni(4s) and $O(2p\sigma)$ orbitals into a (somewhat ionic) σ bond pair with various pairings of the $Ni(3d)^9$ and $O(2p\pi)^3$ configurations. This leads to a number of states, including the ground state, which we find to be $X^3\Sigma^-$. (The electronic structure is analogous to that of O_2.) The calculated D_0 and R_e for the $X^3\Sigma^-$ state of NiO are 89.9 kcal/mol and 1.60 Å, respectively. The bond energy is in good agreement with the experimental value of 86.5 ± 5 kcal/mol, while the R_e value is not known experimentally. The higher group of states involve a doubly occupied $O(2p\sigma)$ orbital. The Ni(4s) orbital in this case is nonbonding and builds in 4p character to move away from the oxygen orbitals. The bonding mainly involves stabilization of the oxygen orbitals by the $Ni(3d)^9$ core (somewhat analogously to the bonding in NiCO). Numerous allowed transitions between these states and the states of the lower group are calculated to be in the range 1.0–3.0 eV, where numerous bands are seen in emission.

I. Introduction

A great deal of attention is currently being directed toward the study of heterogeneous catalysis of various reactions by metal surfaces and homogeneous catalysis using transition metal complexes. A major difficulty in designing and interpreting experimental studies of such systems is that the electronic structure and bonding of unsaturated ligands to transition metals is poorly understood (even at a qualitative level) with very little in the way of quantitative thermochemical data. Indeed, there is currently only very sketchy experimental (or theoretical) information about such simple diatomic systems as transition metal oxides.[3] As part of a project aimed at providing both qualitative and quantitative information about chemisorption and reactions of atoms and molecules on metal surfaces, we carried out a rather extensive study of numerous electronic states of NiO as described herein.

In section II we present the qualitative description of the various states of NiO as obtained from the generalized valence bond (GVB)[6] calculations. Various calculational details are outlined in section III, while section IV describes the details of the configuration interaction (CI calculations). Finally, section V contains a summary of the main results obtained.

II. Qualitative Description

The ground state of $O(^3p)$ has the configuration $(1s)^2(2s)^2(2p)^4$ and can be visualized as in

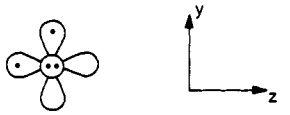

(1)

where

indicates a $2p_z$ orbital in the plane and O indicates a $2p_x$ orbital pointing out of the plane.

Ni is a bit more complicated. Neglecting spin-orbit coupling, the ground state is $^3D(4s^13d^9)$ while the $^3F(4s^23d^8)$ state is at 0.03 eV.[7] Thus, both states could well play a role in the bonding. However, as shown in Figure 1, the 4s orbital of Ni is ~2.5 times larger than the 3d orbitals, so that the bonding is dominated by the 4s orbital. In consequence, the lower bound states of NiO all have essentially $(4s)^1(3d)^9$ character on the Ni.

Before examining the states of NiO we will consider NiH[9] since it illustrates the σ bonding without the complications of the π bonds.

Coupling the $Ni(s^1d^9)$ state to the H leads to an attractive interaction much as in H_2, whereas at large R, coupling the $Ni(s^2d^8)$ state to the H leads to repulsive interactions (arising from the Pauli principle) somewhat analogous to the case of HeH or BeH. At small R the s^2d^8 state can lead to bonding (the atomic state is promoted by splitting the 4s pair into two sp hybrids, one of which overlaps the H); however, the ground state of NiH has the s^1d^9 configuration on the Ni. Allowing the orbitals to readjust, as in the GVB wave function, leads to mixing of small amounts of Ni $4p\sigma$, Ni $3d\sigma$, and H 1s character into the Ni(4s) orbital; however, the qualitative description is as above.

Given that the ground state of NiH has $4s^13d^9$ character on the Ni with the 4s orbital coupled to the H, we expect five low-lying states ($^2\Delta$, $^2\Pi$, and $^2\Sigma^+$) depending on which of the five d orbitals is singly occupied (i.e., which one has the hole). As discussed elsewhere[9] the best state has a δ hole, the next best has a π hole, while the case with a σ hole is worst. The separations here are $\delta \rightarrow \pi$ 0.346 eV and $\delta \rightarrow \sigma$ 0.441 eV. (The effect leading to this ordering is referred to as the intraatomic coupling.[10])

Now we consider NiO. Again we find the lower states to involve a $Ni(4s^13d^9)$ configuration. Assuming this and pairing the Ni(4s) orbital with the singly occupied $O(2p\sigma)$ orbital of (1) leads to five possible Ni $3d^9$ configurations, each of which

0002-7863/78/1500-1338$01.00/0

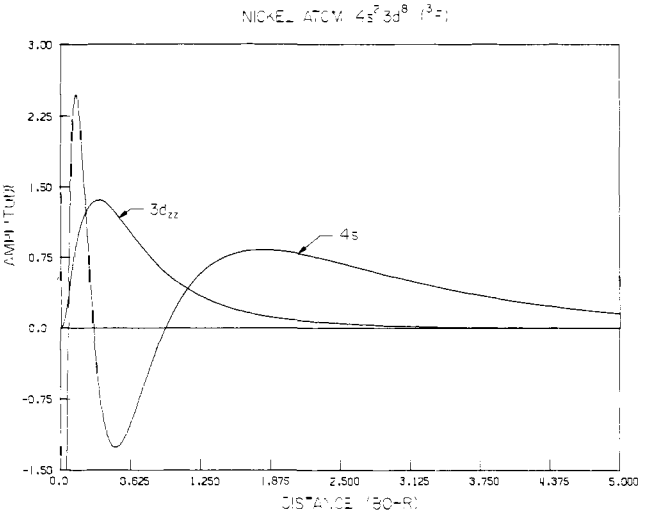

Figure 1. The orbitals of the $^3D(4s^23d^8)$ state of the Ni atom. The orbitals of the $^3D(4s^13d^9)$ state would be indistinguishable from those of the ^3F state in these plots.

can be coupled with two $O(2p\pi)^3$ configurations. Each of these ten spatial configurations leads to a singlet and a triplet, resulting in 20 states (some of which are degenerate) that we will refer to collectively as the group I states.

Pairing the $Ni(4s^13d^9)$ configuration with the oxygen con-

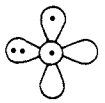

(2)

figuration leads to a number of additional states which generally have a weaker bond owing to repulsive interactions of the $O(2p\sigma)$ doubly occupied orbital with the Ni(4s) orbital. These states lead to bonding because the $O(2p\sigma)$ pair is attracted by the Ni core somewhat as for the CO lone pair in NiCO.[10] The set of states resulting from (2) are denoted as group II states.

A. Group I States. The ten group I configurations corresponding to (1) and the electronic states arising from these configurations are shown below. Each of these configurations involves a σ bond between the Ni(4s) and $O(2p\sigma)$ orbitals, and the ordering of the states is controlled mainly by differences

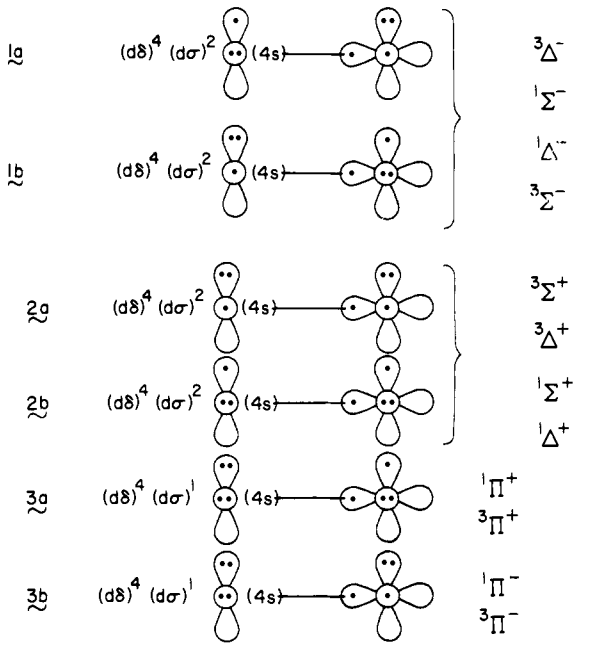

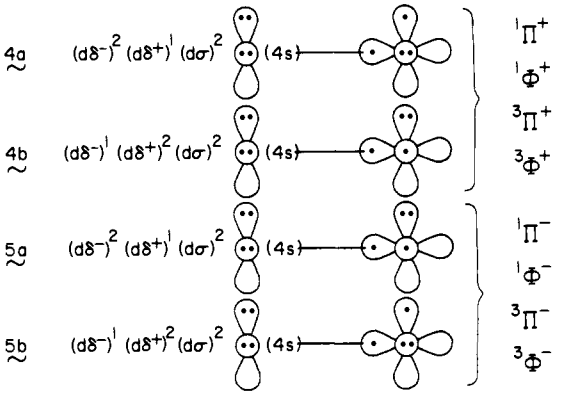

in the π interactions. Thus, we indicate the $Ni(3d\pi)$ and $O(2p\pi)$ orbitals schematically (for simplicity we use the same notation for $Ni(3d\pi)$ orbitals as for $O(2p\pi)$ orbitals) and include the remaining Ni atom configuration in an abbreviated form (e.g., $(d\delta)^4(d\sigma)^2$). In **1–5** the symmetries resulting from each configuration are listed at the right in order of the energy (highest state at the top). (Note that in the following we use + and − designations to indicate symmetry with respect to reflection in the plane of the paper. Thus, π^+ and π^- designations refer to π_y and π_x, respectively.)

Configurations **1** and **2** have a $3d\pi$ hole and lead to states $^3\Sigma^-$, $^1\Delta$, $^1\Sigma^+$, $^1\Sigma^-$, $^3\Delta$, and $^3\Sigma^+$ just as for the analogous case of O_2 (where these six states are the lowest six states). Indeed, the ordering of these states is exactly as in O_2,[11] and we find that the ground state of NiO is the $^3\Sigma^-$ state.

Configurations **3** have a $3d\sigma$ hole and lead to $^{1,3}\Pi$ states. Configurations **4** and **5** (which involve a $3d\delta$ hole) lead to $^{1,3}\Pi$ and $^{1,3}\Phi$ states.

Figure 2 shows the GVB orbitals of configuration **1a** (which together with configuration **1b** leads to the $X^3\Sigma^-$ ground state of NiO). Concentrating first on the σ bond (Figure 2c,d) we see that the $O(2p\sigma)$ component (Figure 2d) of the bond pair is essentially atomic-like, while the Ni(4s) component (Figure 2c) is significantly distorted toward the O. This indicates a somewhat ionic bond (toward the oxygen). These effects are reflected in the Mulliken populations (Table I), which show 0.57 electron transferred from Ni to O.[12] The Ni(4s)-like component of the NiO σ bond pair has incorporated some $3d\sigma$ character.

The relatively large size of the Ni(4s) orbital favors formation of the σ bond at an R much larger than the size of the 3d orbital, leading to small $Ni3d\pi$-$O2p\pi$ overlaps. This is reflected in the localized character of the π orbitals. The doubly occupied $O(2p\pi)$ orbital (Figure 2h) delocalizes somewhat more onto the Ni than does the doubly occupied $Ni(3d\pi)$ orbital (Figure 2e) onto O, leading to a slight net charge transfer back onto the Ni (0.08 electron) in response to the charge flow from Ni to O in the σ system (0.65 electron).

We now consider the ordering of the group I states. Here we first examine the ordering of the covalent configurations **1–5** and then consider modifications to this ordering due to additional configuration interaction (CI) effects.

Consider first configurations **1** and **2**, which lead to states whose ordering is the same as the ordering of the analogous states of the O_2 molecule.[11] In the case of configurations **1**, the singly occupied orbitals are orthogonal leading to the triplet coupling being lower; whereas for configurations **2** the singly occupied orbitals overlap, which leads to the singlet pairing (π bonding) being lower. We now compare the triplet coupling of **1** and the singlet coupling of **2**. Configurations **2** have a single π bond in one direction which is partially counterbalanced by nonbonded interactions between the adjacent doubly occupied orbitals in the other direction. At small R, these repulsive interactions dominate and make **2** unfavorable, whereas

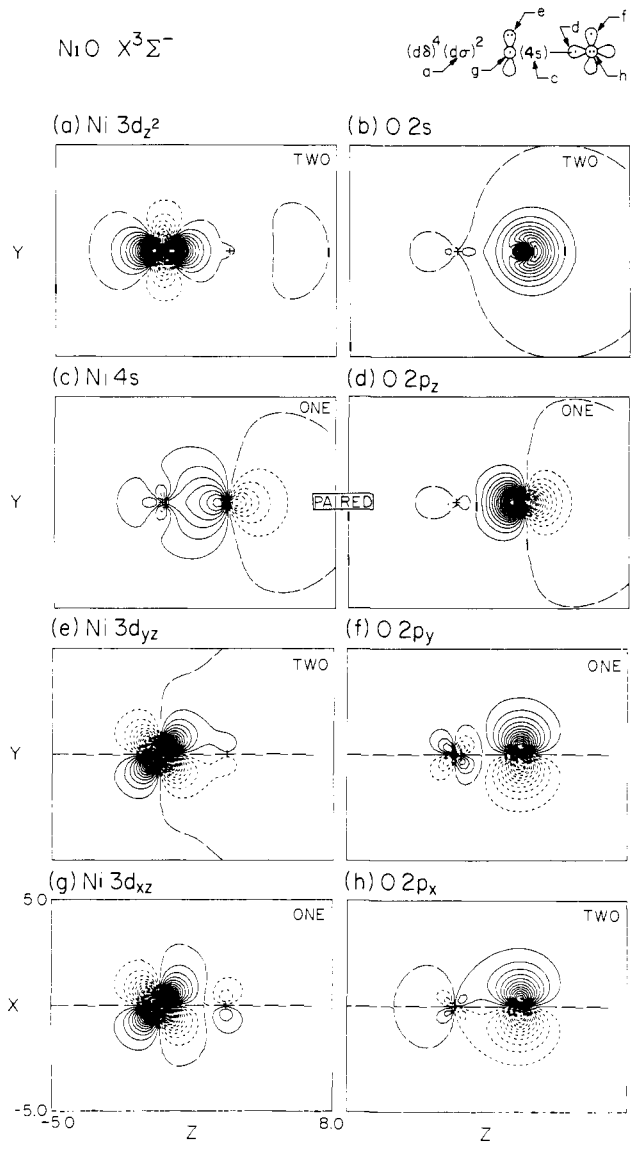

Figure 2. The GVB orbitals of the $X^3\Sigma^-$ state of NiO (at R = 1.63 Å). Unless otherwise noted, all orbital plots have uniformly spaced contours with increments of 0.05 au. Positive contours are indicated by solid lines, negative contours are indicated by dashed lines, and nodal lines are indicated by long dashes. The same conventions are used for the other figures.

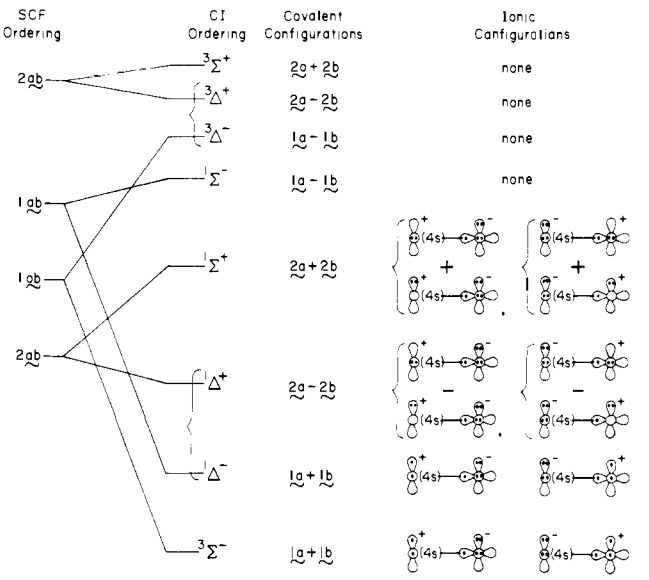

Figure 3. The ordering of the group 1 states of NiO arising from configurations **1** and **2**. The left side indicates the SCF ordering while the right side indicates the CI ordering and the dominant ionic and covalent configurations for each state.

at large R the π bond dominates, favoring **2**. In the case of **1**, there is no π bonding at large R, but at small R the doubly occupied π orbital can delocalize onto the opposite center. This leads to stabilization of the doubly occupied orbital which is partially counterbalanced by antibonding character being introduced into the singly occupied orbitals. The net effect, however, is bonding and is referred to as a three-electron bond.[11]

Thus, **1** should be favorable at large overlap while **2** is favored at small overlap. For O_2, **1** is lower near R_e but the ordering is reversed at large R.[11] Since the $3d\pi$–$2p\pi$ overlap in NiO is small even at R_e (for configuration **2** with a π bond the π overlap is only 0.250 at R = 1.64 Å), we find that for NiO **2** is below **1** for the distances considered here.

Configurations **3**–**5** each involve one three-electron bond, whereas **1** had two three-electron bonds. Thus, based only on the π bonding involved, one expects the ordering

$$\mathbf{2 < 1 < 3 \simeq 4 \simeq 5}$$

However, just as for NiH we expect the states with a $3d\delta$ hole to lead to a stronger σ bond than the states with a $3d\pi$ hole which in turn are more favorable than the states with a $3d\sigma$ hole. Thus, **4** and **5** are stabilized relative to **1** and **2** which in turn are stabilized relative to **3**, leading to the calculated ordering

$$\mathbf{2a < 5b < 1a < 3a}$$

with relative energies of 0.0, 0.064, 0.177, and 0.248 eV, respectively (at R = 1.64 Å).

Thus, the single configurations **1**–**5** are close in energy, and the final ordering is determined by additional CI effects. (In the following we first discuss the states which arise from **1** and **2**.)

Figure 3 shows how configurations **1** and **2** are combined into the $^3\Sigma^-$, $^1\Delta$, $^1\Sigma^+$, $^1\Sigma^-$, $^3\Delta$, and $^3\Sigma^+$ states of NiO and the resultant orderings for SCF and CI wave functions. The left side of Figure 3 shows the ordering of the singlet and triplet couplings of configurations **1** and **2**, while the right side shows the CI ordering and the dominant covalent and ionic configurations involved in the CI wave functions for the various states.

First we consider the SCF ordering. As previously discussed, the singlet coupling of **2** is below the triplet coupling of **1**. We

Table I. Mulliken Populations for the $X^3\Sigma^-$ and $^5\Sigma^-$ States of NiO[a]

	Ni									O						Totals	
State	x^2-y^2	$2z^2-x^2-y^2$	xy	xz	yz	4s	x	y	z	1s	2s	x	y	z	d	Ni	O
$^5\Sigma^-$ (**6**)	2.00	0.92	2.00	1.93	1.93	1.04	0.01	0.01	0.15	2.00	1.94	1.06	1.06	1.94	0.02	9.98	8.02
$X^3\Sigma^-$ (**1**)	2.00	1.76	2.00	1.03	1.97	0.55	0.06	0.02	0.04	2.00	1.92	1.90	1.00	1.73	0.00	9.43	8.57

[a] At R = 1.626 Å, which is close to the equilibrium internuclear separation for the $X^3\Sigma^-$ state of NiO.

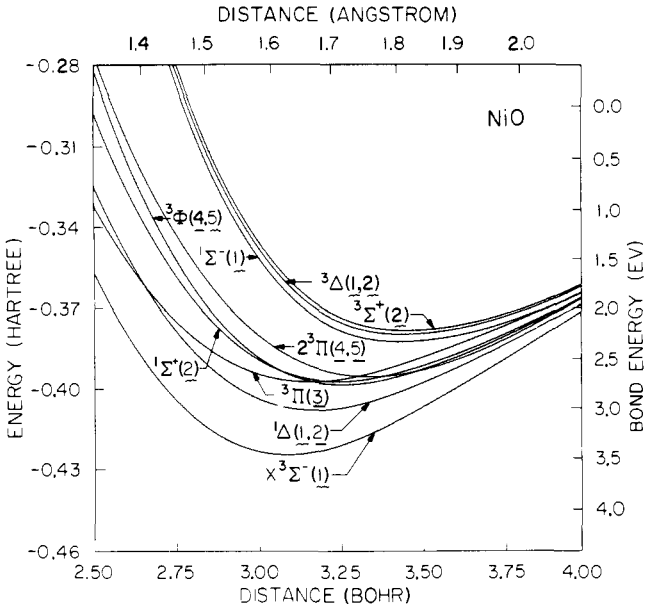

Figure 4. Potential curves for the group I states of NiO based on CI calculations using the $^3\Sigma^-$ basis. The dominant configuration(s) for each state are indicated in parentheses. The singlet states corresponding to **3**, **4**, and **5** were not included in this calculation.

now consider the magnitude of the singlet-triplet splittings for **1** and **2**.

Covalent coupling of two singly occupied orbitals on different centers ϕ_l and ϕ_r leads to singlet and triplet states with energies given by[13]

$$E_S = E_{lr} + \frac{\bar{\tau}}{1 + S^2}$$
$$E_T = E_{lr} + \frac{-\bar{\tau}}{1 - S^2} \qquad (3)$$

where

$$E_{lr} = h_{ll} + h_{rr} + J_{lr}$$
$$\bar{\tau} = 2S\tau + (K_{lr} - S^2 J_{lr})$$
$$\tau = h_{lr} - \frac{1}{2} S(h_{ll} + h_{rr})$$

Here E_{lr} is the energy of the product wave function and the ordering of the singlet and triplet states is determined by the sign of $\bar{\tau}$. If $S = 0$, then $\bar{\tau} = K_{lr} > 0$ and the triplet state is lower (e.g., Hund's rule). If $S \neq 0$, then τ is large and negative and $\bar{\tau}$ is generally negative, leading to a singlet ground state (e.g., H_2 at large R). For **1**, ϕ_l and ϕ_r are orthogonal and the singlet-triplet splitting is given by $2K_{lr}$, which is small. For **2**, ϕ_l and ϕ_r overlap, leading to a large singlet-triplet splitting with singlet lower. Thus we obtain the SCF ordering given in the first column of Figure 3.

The next two columns of Figure 3 show how the covalent configurations **1** and **2** are combined in the various states and the CI ordering of these states (at R_e of the $X^3\Sigma^-$ state).

As shown in the last column of Figure 3, important ionic configurations arise for some states but are excluded (by symmetry) from others; this leads to a large effect upon the relative splittings of the states. Considering first the singlet and triplet couplings of **1**, we see from Figure 3 that the $^1\Delta^-$ and $X^3\Sigma^-$ states have important ionic contributions to the wave function which are not present for the $^3\Delta^-$ and $^1\Sigma^-$ states. Thus, the $X^3\Sigma^-$ and $^1\Delta^-$ states are substantially stabilized with respect to $^3\Delta^-$ and $^1\Sigma^-$. For the singlet coupling of **2**, ionic terms are involved for both the $^1\Sigma^+$ and $^1\Delta^+$ states, leading to comparable energy lowerings for these states and a small splitting, while the states arising from the triplet coupling of **2** do not have important ionic terms.

Table II. GVB Energies from the $X^3\Sigma^-$ and $^5\Sigma^-$ States of NiO[a]

State	$R = 2.7a_0$	$3.0727a_0$	$3.5a_0$	$4.0a_0$	$5.0a_0$
$^5\Sigma^-$ (**6**)	0.237 02	0.296 40	0.314 16	0.311 54	0.299 29
$X^3\Sigma^-$ (**1**)	0.290 42	0.353 21	0.360 04	0.338 75	0.295 24

[a] The quoted number should be subtracted from −115.0 to yield the total energy in hartrees.

Table III. CI Energies for Group I States Using the $^3\Sigma^-$ Basis[a]

Symmetry	$R = 2.7a_0$	$3.0727a_0$	$3.5a_0$	$4.0a_0$	$5.0a_0$
$^3\Sigma^+$ (**2**)[b]	0.259 22	0.357 35	0.379 79	0.362 52	0.316 00
$^3\Delta$ (**1**, **2**)	0.262 47	0.359 57	0.381 14	0.363 23	0.316 16
$^1\Sigma^-$ (**1**)	0.267 28	0.363 14	0.383 82	0.365 51	0.318 95
$2^3\Pi$ (**4**, **5**)	0.332 19	0.387 68	0.395 03	0.367 67	[c]
$^3\phi$ (**4**, **5**)	0.341 50	0.395 04	0.394 92	0.367 62	[c]
$^1\Sigma^+$ (**2**)	0.349 30	0.395 07	0.393 55	0.367 48	0.318 81
$1^3\Pi$ (**3**)	0.369 54	0.398 36	0.390 38	0.365 74	0.316 25
$^1\Delta$ (**1**, **2**)	0.371 28	0.408 41	0.400 07	0.370 02	0.319 12
$X^3\Sigma^-$ (**1**)	0.398 65	0.426 54	0.409 35	0.372 99	0.317 07

[a] The energies are presented in the same form as in Table II. [b] The numbers in parentheses indicate the dominant configurations(s) corresponding to each root. [c] For these cases the Shavitt diagonalization did not converge because the roots are too closely spaced.

For the $X^3\Sigma^-$ state the ionic terms have the effect of allowing delocalization of the doubly occupied π orbitals of **1** onto the other center (i.e., formation of three-electron π bonds). This effect is especially favorable here since the delocalization is in opposite directions in the π_x and π_y systems leading to little net charge transfer. The result is an $X^3\Sigma^-$ ground state for NiO.

For the $^3\Phi$ and $^3\Pi$ states arising from **3**–**5**, ionic configurations involving transfer of a single electron from a Ni($3d\pi$) to an O($2p\pi$) orbital contribute to the wave function. These configurations involve charge transfer from Ni to O which is unfavorable given the ionic NiO σ bond. In addition, they contribute equally to both the $^3\Phi$ and $^3\Pi$ states and thus lead to no net splittings of these states.

Figure 4 shows the potential curves for the group I states of NiO (obtained from CI calculations based on the GVB orbitals of the $X^3\Sigma^-$ state). The CI energies used to construct these curves are given in Table III, while Table II contains the GVB energies of **1a** for comparison. As indicated also in Figure 3, the ordering of the six states with a $3d\pi$ hole is the same as for the corresponding states of O_2. (From the preceding discussion this is expected, since the factors affecting the ordering of these states are analogous to those determining the ordering of the O_2 states.)

Examining now the states arising from a $3d\sigma$ or $3d\delta$ hole, one sees that at small R the $1^3\Pi$ state (which involves a $3d\sigma$ hole) is below the $2^3\Pi$ and $^3\Phi$ states (which involve $3d\delta$ holes), whereas at larger R the ordering is reversed. The ordering at large R is expected since the $3d\delta$ hole is better than the $3d\sigma$ hole for σ bonding. The reversal of $3d\delta$ and $3d\sigma$ at small R seems to arise from a smaller repulsive interaction of the oxygen σ orbitals with the Ni $3d\sigma$ state (one $3d\sigma$ electron) than with the Ni $3d\delta$ state (two $3d\sigma$ electrons); this effect is of negligible importance at large R.

The crossing of the $1^3\Pi$ and $2^2\Pi$ states[14] induces a crossing of the $^3\Phi$ and $2^3\Pi$ states (which each involve a $3d\delta$ hole). At small R the $1^3\Pi$ state is below the $2^3\Pi$ state (although these curves cross, we use the $1^3\Pi$ and $2^3\Pi$ designations as useful mnemonics), hence the lower $1^3\Pi$ state is stabilized, the upper $2^3\Pi$ state is destabilized, while the $^3\Phi$ state is not affected, leading to $^3\Phi$ below $2^3\Pi$. At large R the $2^3\Pi$ state is below the

$1^3\Pi$ state and hence $2^3\Pi$ is stabilized, leading to $2^3\Pi$ below $^3\Phi$.

As discussed in section IIC, there are group II states which overlap the group I $^3\Sigma^-$, $^1\Delta$, and $^1\Sigma^+$ states, leading to incorporation of character of these upper states and further stabilization of these group I states. Including these additional effects leads to a D_0 for the $X^3\Sigma^-$ state of NiO of 89.9 kcal/mol (the D_e value is 91.1 kcal/mol) in good agreement with the experimental bond energy of 86.5 ± 5 kcal/mol.[5] We calculate a NiO bond length of 1.60 Å which, as expected, is a good deal shorter than for bulk NiO (2.08 Å).[15] The bond length for the NiO molecule is not known experimentally.

B. Group II Quintet States. Group II configurations lead to quintet ($S = 2$), triplet ($S = 1$), and singlet ($S = 0$) states. In this section we discuss the simplest of these, the group II quintet states. (The group II singlets and triplets are more complex owing to strong couplings with the group I states.)

Combining the five possible Ni($4s^13d^9$) configurations with the O atom configuration (2) leads to the five group II quintet configurations, **6**, **7**, and **8**, shown below.

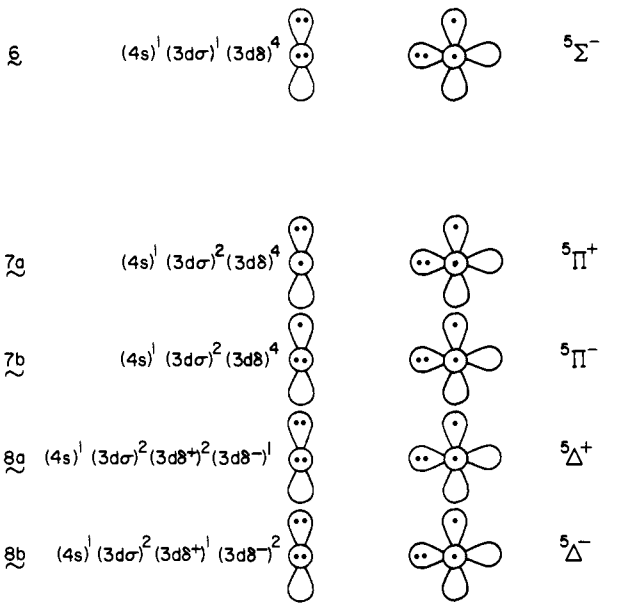

For the group II states the Ni(4s) orbital is nonbonding and simply builds in 4p character to move out of the way of the oxygen orbitals. Since this situation is formally analogous to the bonding of CO to Ni, we compare the bonding here to that in NiCO.[10] In the case of NiCO we found that there was very little delocalization of the C(2s) lone pair of the CO onto the Ni (σ duration), and very little delocalization of the Ni(3d) orbitals onto the CO (π back-bonding). Thus, for CO, the

bonding mainly involves stabilization of the C(2s) orbital by interaction with the partially exposed Ni$(3d)^9$ core. σ donation and π back-bonding effects are of the same order of magnitude as the splittings induced by the intraatomic coupling effect; thus, the lowest state of NiCO has a $3d\delta$ hole and the state having a $3d\sigma$ hole is 0.240 eV higher.

For NiO, however, the high electronegativity of oxygen leads to significant delocalization of the Ni($3d\pi$) orbitals into the singly occupied O($2p\pi$) orbitals. This delocalization is most favorable if it is coupled with delocalization of the doubly occupied O($2p\sigma$) orbital onto Ni in the σ system. Thus, there are important σ-donation π back-bonding effects for the group II NiO states which lead to **6** being the lowest group II quintet state, while **8** is ~1.2 eV higher and **7** should be even higher.

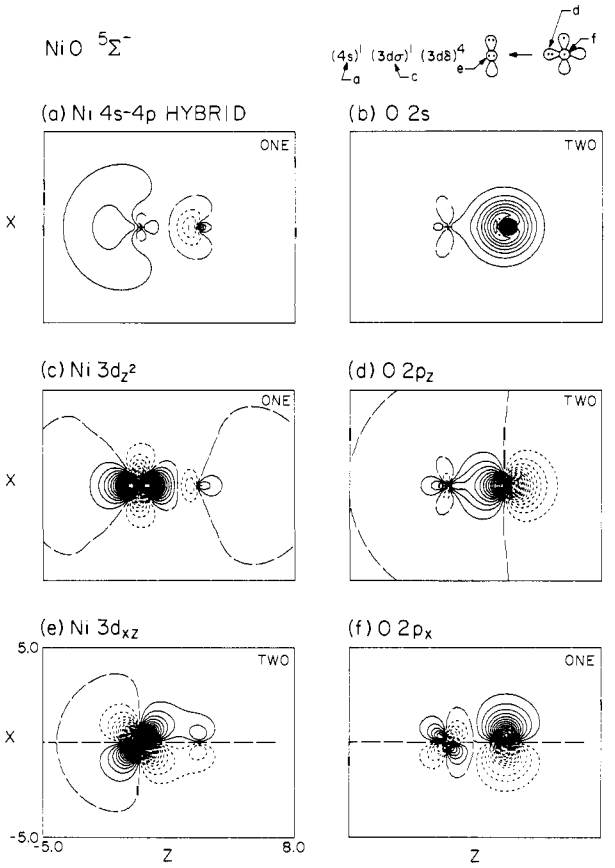

Figure 5. The GVB orbitals of the $^5\Sigma^-$ state of NiO (at $R = 1.63$ Å).

These effects are evident in the orbitals of the $^5\Sigma^-$ state (**6**) which are shown in Figure 5. Here one sees that the Ni(4s) orbital (Figure 5a) has hybridized away from the oxygen while the Ni($3d\pi$) orbitals (Figure 5e) have delocalized substantially onto the oxygen and the doubly occupied O($2p_z$) orbital has delocalized onto the Ni.

The Mulliken populations (Table I) show that the delocalization of the Ni($3d\pi$) orbitals onto O leads to an increase in the total $2p\pi$ population of 0.12, an effect which is counterbalanced by a decrease in the O($2p_z$) population of 0.06, leading overall to a nearly neutral molecule.

In addition to **6–8** there are other important group II quintet states involving ionic configurations. Of these, the states involving a Ni($3d\sigma$) hole are lowest and lead to configurations **9** and **10**, shown below.

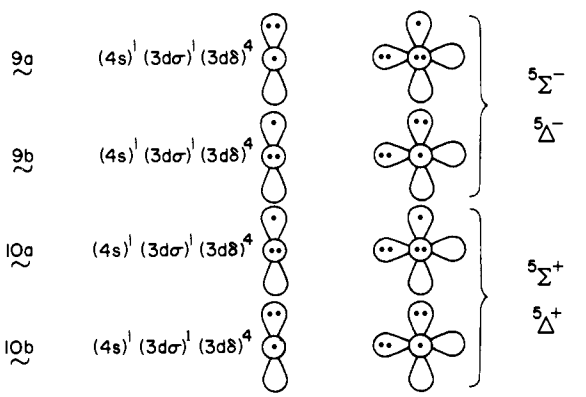

Table IV shows the CI energies for the group II quintet states. These energies are based on CI calculations using the orbitals of **6**. The potential curves for the group II quintet states are shown in Figure 6, along with the potential curves for the group I and group II singlet and triplet states.

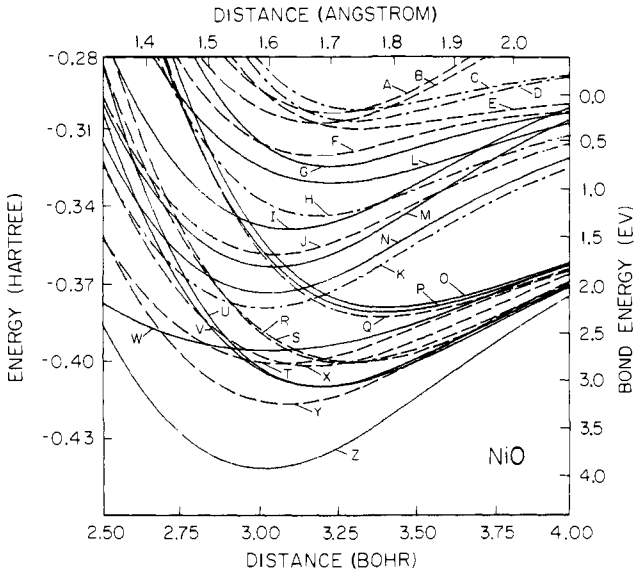

A. $2^1\Sigma^+(11)$ H. $^5\Delta(8)$ O. $^3\Sigma^+(2)$ V. $^3\Phi(4,5)$
B. $2^1\Delta(6,11)$ I. $2^3\Sigma^+(11)$ P. $^3\Delta(1,2)$ W. $^3\Pi(3)$
C. $2^5\Delta(9,10)$ J. $2^1\Sigma^-(6)$ Q. $\Sigma^-(1)$ X. $^1\Sigma^+(2)$
D. $^5\Sigma^+(10)$ K. $^5\Sigma^-(6)$ R. $^1\Phi(4,5)$ Y. $^1\Delta(1,2)$
E. $3^1\Delta(8)$ L. $3^3\Sigma^-(6)$ S. $2^1\Pi(4,5)$ Z. $X^3\Sigma^-(1)$
F. $3^1\Pi(7)$ M. $2^3\Delta(6,11)$ T. $^1\Pi(3)$
G. $3^3\Delta(9,10)$ N. $2^3\Sigma^-(6)$ U. $2^3\Pi(4,5)$

Figure 6. Potential curves for the group I and group II states of NiO based on CI calculations using the $^5\Sigma^-$ POL basis. Singlet states are indicated by dashed lines, triplet states are indicated by solid lines, and quintet states are shown with dot-dashed lines. The dominant configuration(s) for each state are indicated in parentheses.

C. Group II Singlet and Triplet States. The remaining group II states correspond to singlet and triplet couplings of the orbitals in **6–10.** Since some of these states couple strongly with the group I states, the potential curves for these states are based on CI calculations designed to provide a good description of both the group I and group II states (see section IV for a discussion of the details of the CI calculations). The resulting potential curves are those shown in Figure 6 and the energies used to construct these potential curves are tabulated in Tables V and VI.

For the $^5\Sigma^-$ state (**6**), the singly occupied orbitals [Ni(4s), Ni(3dσ), O(2p$_x$), and O(2p$_y$)] are all orthogonal; thus the quintet coupling is lowest. Given these four orthogonal orbitals one can also form three linearly independent triplet states and two linearly independent singlet states,[16] some of which interact strongly with the group I states.

We consider first the triplet states. Singlet coupling of the O(2p$_x$) and O(2p$_y$) orbitals leads to the $^3\Delta^-$ state; two other spin functions can be constructed, both of which have these orbitals triplet coupled, leading to $^3\Sigma^-$ states. Since the exchange integral between the O(2p$_x$) and O(2p$_y$) orbitals is

$2^3\Delta^- =$ | 2p$_x$ 2p$_y$ | 3dσ | 4s | (5)

1.10 eV, whereas the exchange integral between the Ni(3dσ) and Ni(4s) orbitals is only 0.39 eV, the $^3\Delta^-$ state should be highest. This spin coupling is schematically indicated as (5) where vertically adjacent positions indicate high-spin coupling and horizontally adjacent positions indicate singlet coupling (see also ref 16). Using the same notation, the two $^3\Sigma^-$ states are denoted by (6) and (7) while the $X^3\Sigma^-$ state (**1**) has the coupling (8). (Here σ_l and σ_r are the GVB orbitals of the bond pair.) Recombining (6) and (7) we can form one combination (9) which is orthogonal[17] to the ground state and another or-

Table IV. CI Energies for Group II Quintet States Using the $^5\Sigma^-$ Basis[a]

Symmetry	$R = 2.7a_0$	$3.0727a_0$	$3.5a_0$	$4.0a_0$	$5.0a_0$
$2^5\Delta$ (**9, 10**)[b]	0.208 07	0.289 96	0.297 99	0.287 01	
$^5\Sigma^+$ (**10**)	0.211 06	0.294 78	0.301 60	0.287 60	0.282 01
$1^5\Delta$ (**8**)	0.286 30	0.339 58	0.331 89	0.310 40	0.293 94
$^5\Sigma^-$ (**6**)	0.358 79	0.377 68	0.353 49	0.323 07	0.300 71

[a] The energies are presented in the same form as in Table II. [b] See footnote *b* of Table III.

Table V. CI Energies for Group I and Group II Triplet States Using the $^5\Sigma^-$ POL Basis[a]

Group	Symmetry	$R = 2.7a_0$	$3.0727a_0$	$3.5a_0$	$4.0a_0$
II	$3^3\Delta$ (**9, 10**)[b]	0.255 84	0.318 28	0.315 71	0.301 55
II	$3^3\Sigma^-$ (**6**)	0.287 19	0.326 04	0.323 84	0.305 60
II	$2^3\Sigma^+$ (**11**)	0.316 35	0.347 16	0.330 04	0.299 62
II	$2^3\Delta$ (**6, 11**)	0.338 34	0.361 96	0.339 15	0.3031
II	$2^3\Sigma^-$ (**6**)	0.350 99	0.371 98	0.348 88	0.319 14
I	$1^3\Sigma^+$ (**2**)	0.271 17	0.359 74	0.377 14	0.360 27
I	$1^3\Delta$ (**1, 2**)	0.281 60	0.363 22	0.378 77	0.361 05
I	$2^3\Pi$ (**4, 5**)	0.350 39	0.405 80	0.398 31	0.369 15
I	$1^3\Phi$ (**4, 5**)	0.358 69	0.406 12	0.399 44	0.369 74
I	$1^3\Pi$ (**3**)	0.388 00	0.394 59	0.3830	0.360 40
I	$X^3\Sigma^-$ (**1**)	0.421 29	0.440 38	0.413 78	0.373 31

[a] The energies are presented in the same form as in Table II. [b] See footnote *b* of Table III.

Table VI. CI Energies for Group I and Group II Singlet States Using the $^5\Sigma^-$ POL Basis[a]

Group	Symmetry	$R = 2.7a_0$	$3.0727a_0$	$3.5a_0$	$4.0a_0$
II	$2^1\Sigma^+$ (**11**)[b]	0.244 02	0.297 50	0.292 92	0.256 46
II	$3^1\Pi$ (**7**)	0.272 40	0.316 60	0.310 81	0.301 24
II	$2^1\Delta$ (**6, 11**)	0.259 96	0.303 56	0.295 40	0.263 59
II	$2^1\Sigma^-$ (**6**)	0.334 26	0.357 08	0.337 54	0.313 61
I	$2^1\Pi$ (**4, 5**)	0.338 63	0.391 59	0.395 73	0.369 02
I	$1^1\Phi$ (**4, 5**)	0.333 40	0.393 08	0.394 21	0.368 52
I	$1^1\Pi$ (**3**)	0.380 79	0.399 89	0.385 97	0.363 28
I	$1^1\Sigma^-$ (**1**)	0.279 29	0.365 26	0.380 52	0.362 59
I	$1^1\Sigma^+$ (**2**)	0.364 56	0.399 40	0.391 16	0.364 67
I	$1^1\Delta$ (**1**, 2)	0.389 08	0.415 64	0.399 30	0.367 70

[a] The energies are presented in the same form as in Table II. [b] See footnote *b* of Table III.

2p$_x$	3dσ	(6)	2p$_x$	4s	(7)
2p$_y$			2p$_y$		
4s			3dσ		

σ_l	σ_r	(8)
2p$_x$		
2p$_y$		

$2^3\Sigma^- = \sqrt{\frac{2}{3}}$ | 2p$_x$ | 3dσ | 2p$_y$ | 4s | $+ \frac{1}{\sqrt{3}}$ | 2p$_x$ | 4s | 2p$_y$ | 3dσ | (9)

Table VII. Spectroscopic Parameters for the States of NiO[a]

State	D_e, eV	R_e, Å	ω_e,[c] cm^{-1}
	Singlets		
$2^1\Sigma^+$ (**11**)[b]	0.16	1.71	800
$3^1\Pi$ (**7**)	0.50	1.69	737
$2^1\Delta$ (**6, 11**)	0.27	1.69	770
$2^1\Sigma^-$ (**6**)	1.67	1.61	806
$2^1\Pi$ (**4, 5**)	2.81	1.75	695
$1^1\Phi$ (**4, 5**)	2.82	1.73	746
$1^1\Pi$ (**3**)	2.83	1.62	691
$1^1\Sigma^-$ (**1**)	2.33	1.79	684
$1^1\Sigma^+$ (**2**)	2.85	1.68	714
$1^1\Delta$ (**1, 2**)	3.26	1.64	771
	Quintets		
$2^5\Delta$ (**9, 10**)	0.13	1.85	713
$^5\Sigma^+$ (**10**)	0.25	1.83	756
$1^5\Delta$ (**8**)	1.26	1.72	819
$^5\Sigma^-$ (**6**)	2.24	1.63	827
	Triplets		
$3^3\Delta$ (**9, 10**)	0.73	1.71	788
$3^3\Sigma^-$ (**6**)	0.91	1.71	649
$2^3\Sigma^+$ (**11**)	1.40	1.64	809
$2^3\Delta$ (**6, 11**)	1.80	1.61	830
$2^3\Sigma^-$ (**6**)	2.08	1.60	829
$1^3\Sigma^+$ (**2**)	2.23	1.81	667
$1^3\Delta$ (**1, 2**)	2.28	1.80	668
$2^3\Pi$ (**4, 5**)	3.07	1.69	831
$1^3\Phi$ (**4, 5**)	3.07	1.69	775
$1^3\Pi$ (**3**)	2.69	1.60	480
$X^3\Sigma^-$ (**1**)	3.95	1.60	841

[a] Note that within each spin the most strongly bound state is listed at the bottom. [b] See footnote *b* of Table III. [c] ω_e is computed using masses of 16 for O and 58 for Ni.

thogonal component (10) which overlaps the ground state. The ground state incorporates a component of (10) (there is a large matrix element connecting these states since they differ by a single excitation), leading to increased stability and a shorter

$$3^3\Sigma^- = \begin{array}{|c|c|}\hline 3d\sigma & 4s \\ \hline 2p_x & \\ \hline 2p_y & \\ \hline \end{array} = -\frac{1}{\sqrt{3}} \begin{array}{|c|c|}\hline 2p_x & 3d\sigma \\ \hline 2p_y & \\ \hline 4s & \\ \hline \end{array} + \sqrt{\frac{2}{3}} \begin{array}{|c|c|}\hline 2p_x & 4s \\ \hline 2p_y & \\ \hline 3d\sigma & \\ \hline \end{array} \qquad (10)$$

bond length for the $X^3\Sigma^-$ state, while the upper state (10) is pushed up in energy (see Figure 6) thereby rising above the other $^3\Sigma^-$ component (9).[17] The remaining component (5) of $^3\Delta^-$ symmetry is orthogonal to the $1^3\Delta^-$ state, since it involves singlet pairing of the π orbitals, whereas the $1^3\Delta^-$ state has these orbitals triplet coupled.

Consider now the singlet states. The two possible spin couplings of **6** are (11) (where the $2^1\Sigma^-$ state is expected to be

$$2^1\Delta^- = \begin{array}{|c|c|}\hline 4s & 3d\sigma \\ \hline \pi_x & \pi_y \\ \hline \end{array} \qquad 2^1\Sigma^- = \begin{array}{|c|c|}\hline 4s & \pi_x \\ \hline 3d\sigma & \pi_y \\ \hline \end{array} \qquad (11)$$

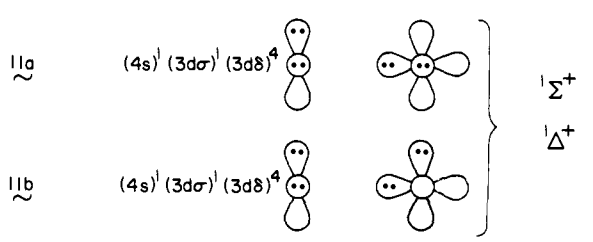

below the $2^1\Delta^-$ state). In addition, configuration **11** leads to $2^1\Sigma^+$ and $2^1\Delta^+$ states. The spin function for the $2^1\Sigma^+$ and $2^1\Delta^+$ states is the same as for the $2^1\Delta^-$ state (these are, of course, degenerate components of the same state) and the $^1\Sigma^+$ and $^1\Delta$ group I states. Thus, just as for the $X^3\Sigma^-$ state these group I states are stabilized by building in components of the group II states and the corresponding group II states are pushed up in energy (see Figure 6). The $2^1\Sigma^-$ state, on the other hand, is orthogonal to the $^1\Sigma^-$ group I state, because its spin function is orthogonal and thus its potential curve is not modified by interaction with the group I states.

Table VIII. Allowed Transitions for NiO[a]

Transition[d]	Energy, eV[c]
Singlet ↔ Singlet Transitions	
$1^1\Delta$ (**1, 2**) ↔ $2^1\Delta$ (**6, 11**)[b]	2.99
$1^1\Delta$ (**1, 2**) ↔ $3^1\Pi$ (**7**)	2.65
$1^1\Sigma^+$ (**2**) ↔ $2^1\Sigma^+$ (**11**)	2.69
$1^1\Sigma^+$ (**2**) ↔ $3^1\Pi$ (**7**)	2.24
$1^1\Pi$ (**3**) ↔ $2^1\Delta$ (**6, 11**)	2.56
$1^1\Pi$ (**3**) ↔ $2^1\Sigma^+$ (**11**)	2.67
$1^1\Pi$ (**3**) ↔ $3^1\Pi$ (**7**)	2.22
$1^1\Pi$ (**3**) ↔ $2^1\Sigma^-$ (**6**)	1.16
$1^1\Phi$ (**4, 5**) ↔ $2^1\Delta$ (**6, 11**)	2.55
$1^1\Phi$ (**4, 5**) ↔ $3^1\Pi$ (**7**)	2.21
$2^1\Pi$ (**4, 5**) ↔ $2^1\Delta$ (**6, 11**)	2.54
$2^1\Pi$ (**4, 5**) ↔ $2^1\Sigma^+$ (**11**)	2.65
$2^1\Pi$ (**4, 5**) ↔ $3^1\Pi$ (**7**)	2.20
$2^1\Pi$ (**4, 5**) ↔ $2^1\Sigma^-$ (**6**)	1.15
Triplet ↔ Triplet Transitions	
$X^3\Sigma^-$ (**1**) ↔ $3^3\Sigma^-$ (**6**)	3.04
$1^3\Pi$ (**3**) ↔ $2^3\Sigma^-$ (**6**)	0.61
$1^3\Pi$ (**3**) ↔ $2^3\Delta$ (**6, 11**)	0.89
$1^3\Pi$ (**3**) ↔ $2^3\Sigma^+$ (**11**)	1.29
$1^3\Pi$ (**3**) ↔ $3^3\Sigma^-$ (**6**)	1.78
$1^3\Pi$ (**3**) ↔ $3^3\Delta$ (**9, 10**)	1.96
$2^3\Pi$ (**4, 5**) ↔ $2^3\Sigma^-$ (**6**)	0.99
$2^3\Pi$ (**4, 5**) ↔ $2^3\Delta$ (**6, 11**)	1.27
$2^3\Pi$ (**4, 5**) ↔ $2^3\Sigma^+$ (**11**)	1.67
$2^3\Pi$ (**4, 5**) ↔ $3^3\Sigma^-$ (**6**)	2.17
$2^3\Pi$ (**4, 5**) ↔ $3^3\Delta$ (**9, 10**)	2.35
$1^3\Phi$ (**4, 5**) ↔ $2^3\Delta$ (**6, 11**)	1.27
$1^3\Phi$ (**4, 5**) ↔ $3^3\Delta$ (**9, 10**)	2.35
$1^3\Delta$ (**1, 2**) ↔ $3^3\Delta$ (**9, 10**)	1.55
Quintet ↔ Quintet Transitions	
$1^5\Delta$ (**8**) ↔ $2^5\Delta$ (**9, 10**)	1.11

[a] The quoted excitation energies are adiabatic. [b] See footnote *b* of Table III. [c] The transition energies correspond to the difference in D_e values; thus they are not corrected for differences in zero point vibrational energy. [d] The following transitions are not allowed because the integral over spin coordinates is zero: $1^1\Sigma^-$ (**1**) ↔ $2^1\Sigma^-$ (**6**), $1^3\Delta$ (**1, 2**) ↔ $2^3\Delta$ (**6, 11**), $X^3\Sigma^-$ (**1**) ↔ $2^3\Sigma^-$ (**6**), $1^3\Sigma^+$ (**2**) ↔ $2^3\Sigma^+$ (**11**).

D. Allowed Electronic Transitions and Properties of the Potential Curves. Energies were calculated at five points over the range 2.7 to $5a_0$ (e.g., see Table III). Cubic splines were fitted to these points for plotting Figure 6, and the resulting R_e, D_e, and ω_e are tabulated in Table VII.

Transitions between group I states or between group II states are expected to be weak, since these are 3d ↔ 3d transitions; however, symmetry-allowed transitions between the two groups of states should be strong, since the group II states are charge transfer states relative to the group I states.[25] Table VIII shows the calculated energies of the 0 ↔ 0 bands for the allowed group I to group II singlet-singlet and triplet-triplet transitions.

Unfortunately, only very sketchy experimental information is available for NiO. The available spectroscopic data come from emission spectra observed in flames or following explosion of nickel wires in the presence of oxygen.[4] The vibrational structure of three bands has been analyzed leading to zero-zero bands at 1.569, 2.036, and 2.620 eV. Numerous other bands

are observed between 1.844 and 2.991 eV. This information is not adequate to make any specific assignments; however, given the transition energies in Table VIII, one would expect a complicated spectrum in the region from about 1.0 to 3.0 eV, as is observed. The vibrational frequencies for those states which have been analyzed fall in the range of ~560 to ~825 cm^{-1}, in the same range as the values calculated.

III. Calculation Details

A. The Modified Effective Potential. In order to carry out calculations of the type described here at reasonable cost, it is expedient to use an effective potential to replace the 18-electron Ar core of the transition metal. Toward this end, Melius, Olafson, and Goddard[18] developed an effective potential, referred to as the ab initio effective potential (AIEP). This AIEP leads to near ab initio accuracy with errors <0.1 eV in excitation energies. However, for the Ni atom ab initio calculations carried out with the usual basis and level of correlation lead to very large errors (2 eV) in the separations of the states. For example, using the Wachters basis,[19] the $s^1d^9(^3D)$ state is calculated in the Hartree-Fock (HF) description to be 2.29 eV above the $s^2d^8(^3F)$ state, whereas the experimental separation is 0.03 eV.[7,8]

The error involved in the usual HF description of the atoms is found to result from (1) a bias in the d basis toward the s^2d^8 state, and (2) differential correlation effects. The basis set problem can be alleviated by addition of another set of 3d primitives ($\alpha \simeq 0.15$) leading to a ^3D-^3F separation of only 1.16 eV. Inclusion of CI effects among the ten valence electrons (but without using f functions) leads to a final energy separation of 0.28 eV.[20] Thus, one approach to obtaining a proper description of molecules involving the Ni atom is to include the extra 3d functions and the CI effects necessary to obtain the proper atomic separations. This is a very expensive and cumbersome procedure for molecules and we have attempted to avoid it. The extra effects necessary to get the correct atomic separations do not lead to significant changes in the shapes of the orbitals in the valence region,[20] and furthermore the necessary correlation effects are *intra*atomic in nature and should be modified only slightly due to bond formation. Thus a simpler but nearly equivalent procedure is to add additional terms to the ab initio effective potential in such a way as to reproduce the atomic separations for HF calculations using the usual Wachter basis, but without significantly altering the orbital shapes. This procedure has been developed by Sollenberger, Goddard, and Melius[9] and the resulting potential is referred to as the modified effective potential (MEP).

The MEP leads to reasonable bond lengths and bond energies for NiH and FeH,[9] and for NiCO,[10] whereas corresponding ab initio calculations lead to very poor results (e.g., no bonding in NiCO). This MEP was used for the calculations described here.

B. Basis Set and Geometry. The basis for Ni was selected from the set optimized for the ground states of the third-row atoms by Wachters.[19] We have used all five d primitives for each of the five types, but, as discussed in ref 18, only the outer four s functions are needed for describing the coreless Hartree-Fock orbital. The inner four d primitives were contracted together and the inner two s functions were contracted together with the relative coefficients based on Hartree-Fock calculations for the $s^2d^8(^3F)$ state of the Ni atom.[9] In addition, a single p primitive with $\alpha = 0.12$ was added in each direction (to allow polarization effects involving the 4s orbital). The final basis for Ni is identical with that used for the NiCO calculations[10] previously reported.

The basis for oxygen is the Dunning (3s, 2p) contraction[22] of the Huzinaga (9s, 5p) basis. This contraction is double ζ for the valence region but uses a single 1s-like contracted function and leads to energies which are generally within 0.0001 hartree of those obtained with the double ζ contraction.[23] The oxygen basis was augmented with a single set of d primitives (orbital exponent $\alpha = 1.04$).

The Ni–O distance was varied from 2.7 to 5.0 bohr.

IV. CI Calculations

As discussed in section II, there are no group I quintet states; thus we were able to describe the group II quintet states by CI calculations using the $^5\Sigma^-$ vectors as a basis. On the other hand, for the group II singlet and triplet states a similar approach leads to two problems: (1) In order for the group II states to be true upper bounds, the lower roots corresponding to the group I states must be adequately represented. (2) Couplings between the group I and group II states are important and are expected to modify both sets of potential curves.

The solution to these problems is to use in the CI an orbital basis capable of describing both sets of states. This approach is developed below. For the group I states, the problem is less serious, in the sense that calculations using the vectors of the $X^3\Sigma^-$ state as a basis do lead to upper bounds to the energy and such calculations were carried out for comparison. (Of course inclusion of the additional group II basis functions and configurations leads to a better description of the group I states and alters the potential curves.)

For the group I CI calculations, the starting point for the CI orbital basis was the set of GVB orbitals for configuration **1a**. Because configuration **1a** is only one of two degenerate configurations describing the $X^3\Sigma^-$ state, the π_x and π_y orbitals were *not* equivalent. In order to generate an equivalent set of π orbitals for the CI, the π_x orbitals were rotated by 90° and combined with the π_y orbitals to obtain two π_x orbitals and two π_y orbitals. To provide sufficient flexibility to describe the excited states, this π space was augmented by adding the more diffuse components of the Ni $3d\pi$ and O $2p\pi$-like functions after orthogonalizing to the previous two π functions. For similar reasons the GVB δ orbitals were augmented by adding the more diffuse δ-like functions (suitably orthonormalized). The resulting basis (referred to hereafter as the $^3\Sigma^-$ basis) consists of 17 functions [including the O(1s)-like function which was kept doubly occupied in all configurations].

The basis for the quintet states was constructed using the GVB orbitals of the $^5\Sigma^-$ state (configuration **6**) and similar procedures for generating the virtuals. This basis (again 17 functions) is referred to hereafter as the $^5\Sigma^-$ basis.

For describing the group I and group II singlet and triplet states simultaneously, the $^5\Sigma^-$ basis was augmented by adding to the basis the $3d\sigma$-like orbital and the GVB natural orbitals of the bond pair from the $X^3\Sigma^-$ state as polarization functions. This basis of 20 functions is referred to as the $^5\Sigma^-$ POL basis. In addition to leading to a good description of the group II singlet and triplet states (as was expected given the origin of the basis), the $^5\Sigma^-$ POL basis was found to lead to *better* energies for some of the group I states (owing to a better description of the ionic group II-like components in those states). The other group I states are described equally well with either this basis or with the $^3\Sigma^-$ basis. Since the $^5\Sigma^-$ POL basis leads to a good description of the potential curves for both sets of states, it was used to generate the potential curves of Figure 6.

The procedure for selecting configurations consisted of selecting a set of generating configurations from which all single excitations into the *full* CI basis were allowed in the final list. The generating configurations for the group I states consisted of products of all possible π orbital occupancies (within the valence orbitals) with the two configurations which arise by allowing single excitations within the two natural orbitals of

Table IX. Generating Configurations for Group I States over the $^3\Sigma^-$ Basis

	Configuration[a]							
	Ni(3dσ)	σ	σ*	Ni(3dπ$_x$)	O(2pπ$_x$)	Ni(3dπ$_y$)	O(2pπ$_y$)	Ni(3dδ$_{xy}$)	Ni(3dδ$_{x2-y2}$)
A1	2	(2 0 / 1 1)[b]	(2 / 1 / 2 / 2 / 0 / 2)	2	1	1	2	2
				1	1	2	2		
				2	2	2	0		
				2	0	2	2		
				0	2	2	2		
				2	2	0	2		
A2	2	(2 0 / 1 1)	(2 / 1 / 1 / 2)	2	1	2	1	2	2
				1	2	1	2		
				1	2	2	1		
				2	1	1	2		
B1	2	(2 0 / 1 1)	(2 / 1)	2	1	2	2	2	1
				1	2	2	2		
	2	(2 0 / 1 1)	(2 / 2)	2	2	2	1	1	2
				2	2	1	2		
	1	(2 0 / 1 1)	(2 / 1)	2	1	2	2	2	2
				1	2	2	2		

[a] σ and σ* are the natural orbitals of the σ bond pair. [b] The parentheses indicate that we take products of the configurations in the left parentheses with those in the right parentheses (e.g., for the A1 case there are 2 × 6 = 12 configurations).

Table X. Generating Configurations for Group II Quintets over the $^5\Sigma^-$ Basis

	Configuration							
	Ni(3dσ)	Ni(4s)	Ni(3dπ$_x$)	O(2pπ$_x$)	Ni(3dπ$_y$)	O(2pπ$_y$)	Ni(3dδ$_{xy}$)	Ni(3dδ$_{x2-y2}$)
A1	1	1	(1 / 2)	1	2	2	2	2
				2	1	1		
	2	1	(2 / 1 / 1 / 2)	1	2	1	1	2
				2	1	2		
				2	2	1		
				1	1	2		
	2	1	(1 / 2)	1	2	2	2	1
				2	1	1		
A2	1	1	(2 / 1 / 2 / 1)	1	2	1	2	2
				2	1	2		
				1	2	1		
				2	1	2		
	2	1	(1 / 2)	1	2	2	1	2
				2	1	1		
	2	1	(2 / 1 / 2 / 1)	1	1	2	2	1
				2	2	1		
				1	2	1		
				2	1	2		
B1	2	1	(2 / 1 / 2 / 2)	1	1	1	2	2
				2	1	1		
				1	2	0		
				2	1	2		

the σ bond pair, for each of the five possible choices for the hole in the Ni(3d) shell. (A similar procedure was used for the group II states.) This set of configurations can also be obtained by allowing all single excitations from the reference configurations (**1–5**). Thus, the final CI contained single and double excitations within the valence space and single excitations into the virtual space (with respect to the reference configurations).

The procedure is analogous to the approach which Moss and Goddard[11] found to lead to a good description of the states of O_2 and is essentially equivalent to the POL-CI-1 method of Dunning and Hay.[24] It differs from the POL-CI method[24] in that it excludes certain double excitations which consist of products of a single excitation in the valence space and an excitation into a virtual orbital.

Table IX shows the generating configurations for the group I states over the $^3\Sigma^-$ basis. Allowing single excitations from the generating configurations into the full CI basis led to (130, 232), (92, 208), (122, 326), (92, 324), (158, 626) [(spatials, spin eigenfunctions)] for the $^1A_1$, $^1A_2$, $^3A_1$, $^3A_2$, and $^3B_1$ CIs, respectively.

Table X shows the generating configurations for the group II quintet states over the $^5\Sigma^-$ basis. Allowing all singles from the generating configurations into the full CI basis led to (106, 242) and (128, 280) [(spatials, spin eigenfunctions)] for the $^5A_1$ and $^5A_2$ CIs, respectively.

Table XI shows the generating configurations used for the singlet and triplet group I and group II states using the $^5\Sigma^-$ POL basis. From these generating configurations all singles were allowed among the GVB orbitals plus the π- and δ-like virtuals. For the starred configurations (which have group I character) we also allowed all singles into the σ virtuals (obtained from the group I orbitals). This led to (410, 852), (320, 826), (278, 982), (398, 1282), (320, 1332), and (378, 1586) [(spatials, spin eigenfunctions)] for the $^1A_1$, $^1A_2$, $^1B_1$, $^3A_1$, $^3A_2$, and $^3B_1$ CIs, respectively.

V. Summary

We find that the low-lying states of NiO all involve the s^1d^9 (^3D) configuration of the Ni atom and lead to two groups of states (denoted as group I and group II, respectively). The group I states involve O atom configurations with a singly

Table XI. Generating Configurations for Group I and Group II Singlets and Triplets over the $^5\Sigma^-$ POL Basis

	Configuration								
	O(2pσ)	Ni(3dσ)	Ni(4s)	Ni(3dπ$_x$)	O(2pπ$_x$)	Ni(3dπ$_y$)	O(2pπ$_y$)	Ni(3dδ$_{xy}$)	Ni(3dδ$_{x2-y2}$)
A1	(2 2 1)[a]	1 2 1	1 0* 1*	(2 2 2 2 0 2)	2 1 0 2 2 2	1 2 2 2 2 0	1 2 0 2 2 2	2	2
	2	2	1	(2 1 2 1)	1 2 1 2	1 2 2 1	2 1 1 2	1	2
	2	2	1	(2 1 2 2 0)	2 1 2 2 2	1 2 2 0 2	1 2 2 2 2	2	1
A2	(2 2 1)	1 2 1	1 0* 1*	(2 2 1 2)	1 2 1 2	1 2 2 1	2 1 1 2	2	2
	2	2	1	(2 2 1 2 0)	2 2 1 1 2	2 2 2 0 2	2 1 2 2 2	1	2
	2	2	1	(2 1 2 1)	1 2 1 2	1 2 2 1	2 1 1 2	2	1
B1	(2 1 2)	1 1 0	0* 1* 1	(2 1)	2 2	2 2	2 2	2	2
	2	2	1	(2 1 2 2)	1 2 1 2	1 1 2 1	1 1 0 2	2	2
	(2 2 1)	2 1 2	0* 1 1*	(2 2 2)	2 2 1	2 1 2	1 2 2	1 2 2	2 2 1
				1	2	2	2	2	1

[a] See footnote *b* of Table IX.

occupied O(2pσ) orbital leading to formation of a covalent σ bond with the singly occupied Ni(4s) orbital. The remaining 3d hole may be taken in a 3dσ, 3dπ, or 3dδ orbital, respectively. The 3dπ hole leads to $^3\Sigma^-$, $^1\Delta$, $^1\Sigma^+$, $^1\Sigma^-$, $^3\Delta$, and $^3\Sigma^+$ states, analogous to the corresponding states of O_2, while the 3dσ hole leads to $^{1,3}\Pi$ states and the 3dδ hole leads to $^{1,3}\Pi$ and $^{1,3}\Phi$ states. We find that the ground state of NiO is the $^3\Sigma^-$ state which has an electronic structure analogous to the ground state of O_2. The D_0 and R_e values for the ground state are 89.9 kcal/mol and 1.60 Å, respectively. The D_0 value is in good agreement with the experimental value of 86.5 ± 5 kcal/mol, while the R_e value for NiO is not known experimentally.

The group II states involve an O atom configuration where the O(2pσ) orbital is doubly occupied. The Ni(4s) orbital here is nonbonding and builds in 4p character to move away from the oxygen orbitals. The bonding is somewhat analogous to the bonding in NiCO, but the high electronegativity of oxygen leads to substantial delocalization of the doubly occupied Ni(3dπ) orbitals onto oxygen simultaneous with delocalization of the doubly occupied O(2pσ) orbital onto Ni. Thus the $^5\Sigma^-$ state with a 3dσ hole is lowest.

Taking the singlet and triplet couplings of the orbitals of the group II quintet states leads to other group II states some of which are strongly coupled with the group I states, leading to stabilization of certain group I states and concomitant destabilization of certain group II states. Since the group II states are charge transfer states relative to the group I states, allowed transitions between the two sets of states should be strong leading to the prediction of numerous allowed transitions in the energy range of ~1.0 to ~3.0 eV (in the range where emission bands are observed).

References and Notes

(1) Partially supported by a grant (DMR74-04965) from the National Science Foundation.
(2) Acknowledgment is made to the donors of the Petroleum Research Fund, administered by the American Chemical Society, for partial support of this research.
(3) For NiO some spectroscopic information is available from the analysis of emission spectra, as summarized in ref 4. The bond energy is known (ref 5).
(4) B. Rosen, "Tables of Constants and Numerical Data", S. Bourcier, Ed., Pergamon Press, Oxford, 1970.
(5) R. T. Grimley, R. P. Burns, and M. G. Ingraham, *J. Chem. Phys.*, **35**, 551 (1961).
(6) W. A. Goddard III, T. H. Dunning, Jr., W. J. Hunt, and P. J. Hay, *Acc. Chem. Res.*, **6**, 368 (1973).
(7) The quoted atomic separations are obtained by taking a weighted average over the spectral levels corresponding to a given L and S (spin–orbit interactions are not included in our calculations). The values are from ref 8.
(8) C. E. Moore, "Atomic Energy Levels", Vol. II, National Bureau of Standards, Washington, D.C., 1952.
(9) M. J. Sollenberger, Masters Thesis, California Institute of Technology, 1975; C. F. Mellus, W. A. Goddard III, and M. J. Sollenberger, to be published.
(10) S. P. Walch and W. A. Goddard III, *J. Am. Chem. Soc.*, **98**, 7908 (1976).

(11) For a discussion of the states of O_2 see B. J. Moss and W. A. Goddard III, *J. Chem. Phys.*, **63**, 3523 (1975); B. J. Moss, F. W. Bobrowicz, and W. A. Goddard III, *ibid.*, **63**, 4632 (1975).
(12) This is from Mulliken populations. Generally, these populations indicate a greater charge transfer than would be indicated, for example, by the dipole moment. Thus, the populations, although indicative of relative charge transfer, should not be taken too literally.
(13) The discussion here is related to the approach used by C. W. Wilson, Jr., and W. A. Goddard III, *Chem. Phys. Lett.*, **5**, 45 (1970); *Theor. Chim. Acta*, **26**, 195, 211 (1972).
(14) In Figures 4 and 6 we draw the $1^3\Pi$ and $2^3\Pi$ states as crossing. Actually, there is a matrix element connecting them which leads to a small energy gap and adiabatic states which do not cross.
(15) E. I. Alessandrini and J. F. Freedman, *Acta Crystallogr.*, **16**, 54 (1963); G. W. C. Wyckoff, "Crystal Structures", 2nd ed, Interscience, New York, N.Y., 1964.
(16) The spin eigenfunctions (SEFs) used are as follows. For the four-electron singlet

$$G1 = a[\phi_1\phi_2\phi_3\phi_4 \frac{1}{\sqrt{4}}\{(\alpha\beta - \beta\alpha)(\alpha\beta - \beta\alpha)\}] = \begin{array}{|c|c|}\hline \phi_1 & \phi_2 \\ \hline \phi_3 & \phi_4 \\ \hline \end{array}$$

$$G2 = a[\phi_1\phi_2\phi_3\phi_4 \frac{1}{\sqrt{12}}\{2\alpha\alpha\beta\beta + 2\beta\beta\alpha\alpha - (\alpha\beta + \beta\alpha)(\alpha\beta + \beta\alpha)\}] = \begin{array}{|c|c|}\hline \phi_1 & \phi_3 \\ \hline \phi_2 & \phi_4 \\ \hline \end{array}$$

For the four-electron triplet

$$G1 = a[\phi_1\phi_2\phi_3\phi_4 \frac{1}{\sqrt{2}}\{(\alpha\beta - \beta\alpha)\alpha\alpha\}] = \begin{array}{|c|c|}\hline \phi_1 & \phi_2 \\ \hline \phi_3 \\ \cline{1-1} \phi_4 \\ \cline{1-1} \end{array}$$

$$G2 = a[\phi_1\phi_2\phi_3\phi_4 \frac{1}{\sqrt{6}}\{2\alpha\alpha\beta\alpha - (\alpha\beta + \beta\alpha)\alpha\alpha\}] = \begin{array}{|c|c|}\hline \phi_1 & \phi_3 \\ \hline \phi_2 \\ \cline{1-1} \phi_4 \\ \cline{1-1} \end{array}$$

$$G3 = a[\phi_1\phi_2\phi_3\phi_4 \frac{1}{\sqrt{12}}\{3\alpha\alpha\alpha\beta - (\beta\alpha\alpha + \alpha\beta\alpha + \alpha\alpha\beta)\alpha\}] = \begin{array}{|c|c|}\hline \phi_1 & \phi_4 \\ \hline \phi_2 \\ \cline{1-1} \phi_3 \\ \cline{1-1} \end{array}$$

where horizontally coupled orbitals indicate that the spin function is asymmetric under interchange of *a* and *b*, while vertically coupled orbitals indicate that the spin function is symmetric under interchange of *a* and *b*.
(17) Since the SEFs are orthogonal, states corresponding to different spin eigenfunctions (SEFs) can at most be coupled by transpositions arising from the antisymmetrizer. The resulting matrix elements involve two-electron exchange integrals and are generally smaller than for cases where the two states have the same SEF (in which case they can have one-electron terms connecting them, if they differ by only a single excitation).
(18) C. F. Melius, B. D. Olafson, and W. A. Goddard III, *Chem. Phys. Lett.*, **28**, 457 (1974); C. F. Melius and W. A. Goddard III, *Phys. Rev. Sect. A*, **10**, 1528 (1974).
(19) A. J. H. Wachters, *J. Chem. Phys.*, **52**, 1033 (1970).
(20) T. A. Smedley and W. A. Goddard III, unpublished calculations. Similar effects have been observed by Brooks and Schaefer for the Mn atom (ref 21).
(21) B. R. Brooks and H. F. Schaefer III, "A Model Transition Metal-Carbene System $MnCH_2$", to be published.
(22) T. H. Dunning, Jr., and P. J. Hay in "Modern Theoretical Chemistry: Methods of Electronic Structure Theory", Vol. 3, H. F. Schaefer III, Ed., Plenum Press, New York, N.Y., 1977. The p functions are the same as in ref 23, the tightest seven s functions are contracted into a single s function based on the 1s HF orbital, the second and third most diffuse are contracted into a basis function based on the 2s HF orbital, and the most diffuse function is uncontracted.
(23) T. H. Dunning, Jr., *J. Chem. Phys.*, **53**, 2823 (1970).
(24) P. J. Hay and T. H. Dunning, Jr., *J. Chem Phys.*, **64**, 5077 (1976).
(25) The group II states of NiO are analogous to the Shumann–Runge states of O_2 which involve transfer of one electron from one oxygen atom to the other in the σ system coupled with transfer of a second electron in the opposite direction in the π system. Thus, we refer to the group II states as charge

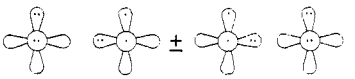

transfer states relative to the group I states even though both sets of states arise from neutral atomic configurations.

Dissociation Energies, Electron Affinities, and Electronegativities of Diatomic Molecules. An Empirical Correlation with Predictions for XY, XY^+, and XY^-

William F. Sheehan

Contribution from the Department of Chemistry, University of Santa Clara, Santa Clara, California 95053. *Received October 8, 1976*

Abstract: Experimental dissociation energies D_0 of diatomic molecules containing elements from Li to F and Na to Cl have been correlated empirically by imagining a continuous two-dimensional function in atomic-number space. Contours of constant $D_0(XY)$ and $D_0(XY^+)$ show remarkable similarities that allow prediction of dissociation energies of uninegative ions XY^-. From $D_0(XY^+)$ and $D_0(XY^-)$, electronegativities and electron affinities of XY are calculated for diatoms of Li to F. The method is readily extended to other elements.

Introduction

Dissociation energies $D_0(XY)$ of many diatomic molecules XY have been determined, some with exceptional accuracy. Recent lists[1] of such values seem to reach a best or recommended value by thorough study of all data for a particular diatom with perhaps some subjective estimate of general reasonableness or physical limits in the background. The mass of data that are reliable has grown through the years until now, for diatoms made of elements from Li to F and from Na to Cl, only a relatively few values remain absent.

This paper presents an empirical correlation of the D_0s of Tables I and II. All the values are experimental. It seemed best from the start to exclude all calculated values, not because all are unreliable, but merely because there is a clear distinction between what is observed and what is calculated. However, in accord with theory, the elusive $D_0(Be_2)$ has been assumed to be essentially zero, as have D_0s for all diatoms with four valence electrons.

Computational Details

Tables I and II list D_0s by atomic numbers of the atoms. When these values are listed in square arrays according to atomic number, regular trends are evident. Irregularities, obvious in the array, are expected theoretically because of the quantized energies of both atoms and molecules, yet it is possible to find effectively continuous contours of constant energy.

0002-7863/78/1500-1348$01.00/0